Continuity and Stability of families of figure eight orbits with finite angular momentum.

Michael Nauenberg
Department of Physics
University of California, Santa Cruz, CA 95064

Abstract

Numerical solutions are presented for a family of three dimensional periodic orbits with three equal masses which connects the classical circular orbit of Lagrange with the recently discovered planar figure eight orbit with zero total angular momentum [1],[2]. Each member of this family is an orbit with finite angular momentum that is periodic in a frame which rotates with frequency Ω around the horizontal symmetry axis of the figure eight orbit. Numerical solutions for figure eight shaped orbits with finite angular momentum orbits were first reported in [3], and mathematical proofs for the existence of such orbits were given in [5], and more recently in [6] where also some numerical solutions have been presented. Numerical evidence is given here that the family of such orbits is a continuous function of the rotation frequency Ω which varies between $\Omega = 0$, for the planar figure eight orbit with intrinsic frequency ω, and $\Omega = \omega$ for the circular Lagrange orbit. Similar numerical solutions are also found for $n > 3$ equal masses, where n is an odd integer, and an illustration is given for $n = 21$. Finite angular momentum orbits were also obtained numerically for rotations along the two other symmetry axis of the figure eight orbit [3], and some new results are given here. Recently, existence proofs for families of such orbit and further numerical solutions have been given in [6]. The stability of these orbits is examined numerically without the restriction to a linear approximation [6], and some examples are given of nearby stable orbits which bifurcate from these families.

Introduction

In 1993 C. Moore [1] discovered a new periodic orbit for three particles of equal mass moving synchronously on a symmetric planar figure eight orbit under the action of their mutual attractive gravitational forces. Subsequently, a mathematical proof for the existence of this orbit and an accurate numerical solution were given in [2]. This orbit has total angular momentum equal to zero. Similarly shaped figure eight orbits with finite angular momentum were obtained numerically, and were first presented in [3]. Before Moore's discovery, C. Marchal[4] had obtained a perturbative orbit in the shape of a three dimensional figure eight which bifurcates from the classical Lagrange orbit for three equal masses located on the vertices of an equilateral triangle which rotates uniformly around its center. This perturbed orbit is periodic in a frame rotating around an axis normal to the plane and through the center of the Lagrange orbit, with a small rotation angular frequency proportional to the square of the maximum amplitude of the perturbation amplitude along this axis. After learning about the existence of the planar figure eight orbit, Marchal gave a proof [5] for the existence of a family of three dimensional orbits where each member is periodic in a frame rotating around the horizontal symmetry axis of the planar figure eight orbit. This family connects the figure eight orbit to a Lagrange orbit, with its plane normal to this axis, by varying the angular rotation frequency Ω of this frame. Both the perturbative orbit that bifurcates from the Lagrange orbit [4],[5], and the finite angular momentum orbit that bifurcates from the figure eight orbit along the horizontal axis of symmetry [3], are members of this family. Numerical solutions of periodic orbits that bifurcate from the figure eight in a frame rotating around an axis normal to its horizontal symmetry axis, were also reported in [3]. Recently, another proof for the existence of such periodic orbits and some numerically generated figures for these orbits were given in reference [6]. But a proof has not been given for the *continuity* as a function of the rotation frequency Ω of the family of periodic orbits between the Lagrange orbit and the planar figure eight orbit. In reference [5], Marchal concluded that " the next step will be of course... the numerical verification of the continuity up to the eight shaped orbit... ". Moreover, the stability of these orbits have been examined only in a linear approximation [6], but this turns out to be inadequate, as will be shown here.

In this paper, we extend previous numerical results [3], [6], and show

numerically that the family of three dimensional orbits which connects the classical circular orbit of Lagrange with the planar figure eight orbit is a continuous function of the angular rotation frequency Ω of a frame rotating around the horizontal symmetry axis of the figure eight, where the orbits are periodic. These orbits are obtained by expanding its coordinates in this rotating frame in a Fourier series, and calculating the Fourier coefficients by a steepest descent gradient method [3] discussed in section I. The first nine coefficients for this expansion are given in Figs. 4-6, which provides numerical evidence that as a function of the rotation frequency Ω of this frame (with fixed frequency $\omega = 1$ of the periodic orbit), the coefficients vary continuously between those for the planar figure eight orbit for $\Omega = 0$, and those for the Lagrange orbit at $\Omega = 1$. In particular, we verify numerically that in these two limits, the Fourier coefficients approach the values obtained from these perturbative solutions. Marchal evaluated the first few orders for the perturbative solution near the Lagrange orbit, which can be expressed as a series in powers of the *square root* of the rotation frequency Ω [4],[5]. The corresponding perturbation solution near the zero angular momentum figure eight orbit is in powers of Ω, as was pointed out in [3]. In Fig. 7 we provide evidence that the numerical derivative of the first three Fourier coefficients also does not have discontinuities.

The convergence of a finite Fourier sum to an approximate solution of the equations of motion can be verified numerically, to a given accuracy, by comparing the Fourier sum for the acceleration with the corresponding sum for the total force acting on each mass, including the centrifugal and coriolis force in the rotating frame. In our work we found that to get agreement between these two quantities to and accuracy of 10^{-5} it is sufficient to keep only terms in the Fourier sum up to $k = 27$ or $k = 28$. Since either even or odd terms in these sums vanish, this represents only 14 terms in these sums. To the same accuracy, we have verified that the Fourier sum for the total energy and the total angular momentum about the rotation axis are constants. Moreover, the convergence of the Fourier sum has also been verified by comparing it with a direct numerical integration of the equations of motion with a fourth order Runge-Kutta algorithm, with initial conditions obtained from the Fourier expansion.

In section II we illustrate the application of the Fourier gradient method near the classical Lagrange solution by a first order perturbation calculation similar to Marchal's. As is well known, this solution can be extended to

any odd number n of equal masses on the vertices of a regular nth polygon, and this is also the case for the figure eight shaped orbit, as was shown numerically in [3], [7]. Likewise, we have found that the family of periodic orbits connecting these two orbits can also be extended to an odd number of masses. As an illustration, we present in Fig. 2 numerical results for the case that $n = 21$. Some additional numerical solutions for finite angular momentum orbits associated with rotations of the planar figure eight orbit along the y and z axes of symmetry [3] [6] are shown in Figs. 7-9. These results are discussed in section III. Finally, in section IV we examine the stability of these families of orbits by integrating the equations of motion numerically with a fourth order Runge-Lenz algorithm, taking for initial conditions values of the coordinates and momenta nearby to those obtained previously with our Fourier gradient method for periodic solutions.

I. Fourier gradient method

The symmetry properties of the periodic planar figure eight shaped orbit for three equal masses [1],[2],[5] dictate the form of the Fourier series expansion of the orbital coordinates. For Newtonian gravitational interactions, the coordinate and the time scale according to the Keplerian transformation $x(t) = \tau^{2/3} f(t/\tau)$, where τ is the period; and similarly for the $y(t)$ coordinate. Choosing for convenience $\tau = 2\pi$, we have

$$x(t) = \sum_{k=1}^{\infty} a(k_o) sin(k_o t), \tag{1}$$

$$y(t) = \sum_{k=1}^{\infty} b(k_e) sin(k_e t) \tag{2}$$

where $k_o = 2k - 1$ and $k_e = 2k$. This represention is also valid for any odd number $n \geq 3$ of equal masses, where the position of the jth mass at time t is given by $x_j(t) = x(t + j\tau/n)$ and $y_j(t) = y(t + j\tau/n)$ for $j = 0, ..(n-1)$. The conservation of total linear momentum requires that the Fourier coefficients $a(k_o)$ and $b(k_e)$ vanish for k_o mod n and k_e mod $2n$ respectively. For a figure eight shaped orbit with finite angular momentum about the x or y axis of symmetry, this expansion remains valid in a frame rotating around one of these symmetry axes, but then the orbit depends also on the coordinate z normal to the $x - y$ plane in the rotating frame. For the case of rotations

around the x axis, it can be readily shown from the equations of motion that the Fourier expansion of $z(t)$ has the form

$$z(t) = \sum_k c(k_e) cos(k_e t), \tag{3}$$

while for rotations around the y axis

$$z(t) = \sum_k c(k_o) cos(k_o t). \tag{4}$$

In the fixed frame, the corresponding coordinates can conveniently be obtained by introducing complex variables. For example, for rotation around the x axis, we have

$$x_j(t) = \sum_k sin(k_o(t + 2\pi j/n)), \tag{5}$$

and

$$y_j(t) + iz_j(t) = e^{i\Omega t} \sum_k e^{ik_e(t+2\pi j/n)}(b(k_e) + ic(k_e)), \tag{6}$$

where Ω is the angular rotation frequency of the frame. Setting $\Omega = 1 - \beta$ for $0 \leq \Omega$ and $\Omega = -1 + \beta$ for $\Omega \leq 0$, we see that an orbit which is periodic in the coordinate rotating with angular frequency Ω is also periodic in another frame rotating with angular frequency β. For $n = 3$ and $\Omega = -1 + \beta$, this representation corresponds to that given by Marchal [4],[5], where β is the angular rotation frequency of a frame relative to which the Lagrange orbit has period 2π,

We evaluate these Fourier coefficients by determining the extrema of the action integral A for an orbit given by Eqs. 1-4 in a frame rotating with angular frequency Ω. For example, for the case that the axis of rotation is taken along the x axis of symmetry of the planar figure eight orbit, we have

$$A = \int_0^{2\pi} dt[K(t) - P(t) + \frac{1}{2}\Omega^2 I_x(t) + \Omega L_x(t)], \tag{7}$$

where $K(t)$ is the kinetic energy, $P(t)$ the potential energy, $I_x(t)$ the x-moment of inertia, and $L_x(\theta)$ the x component of angular momentum in this rotating frame. These dynamical variables are given by the following expressions:

$$K(t) = \frac{1}{2}\omega^2 \sum_{j=1}^{j=n} (\frac{dx_j}{dt})^2 + (\frac{dy_j}{dt})^2 + (\frac{dz_j}{dt})^2, \tag{8}$$

$$P(t) = -\sum_{i,j} \frac{1}{r_{ij}(t)^3}, \tag{9}$$

where $r_{ij}(t) = \sqrt{(x_i(t) - x_j(t))^2 + (y_i(t) - y_j(t))^2 + (z_i(t) - z_j(t))^2}$ is the distance between particles i and j,

$$I_x(t) = \sum_{i=1}^{i=n} y_(t)_i^2 + z_i(t)^2, \tag{10}$$

is the moment of inertia, and

$$L_x(t) = \omega \sum_{i=1}^{i=n} y_i(t) \frac{dz_i(t)}{dt} - z_i(t) \frac{dy_i(t)}{dt} \tag{11}$$

is the angular momentum. The extrema of the action integral, Eq. 7, is obtained by determining the Fourier coefficients for which the partial derivatives of the action with respect to these coefficients vanish [3],

$$\frac{\partial A}{\partial a(k_o)} = u(k_0)a(k_o) - f(k_o) = 0, \tag{12}$$

$$\frac{\partial A}{\partial b(k_e)} = u(k_e)b(k_e) - g(k_e) + v(k_e)c(k_e) = 0, \tag{13}$$

$$\frac{\partial A}{\partial c(k_e)} = u(k_e)c(k_e) - h(k_e) + v(k_e)b(k_e) = 0, \tag{14}$$

where $u(k) = k^2\omega^2 + \Omega^2$ and $v(k) = 2k\omega\Omega$, and

$$f_(k) = \frac{1}{\pi} \int_0^{2\pi} dt \frac{\partial P}{\partial x} sin(kt), \tag{15}$$

$$g(k) = \frac{1}{\pi} \int_0^{2\pi} dt \frac{\partial P}{\partial y} sin(kt), \tag{16}$$

$$h(k) = \frac{1}{\pi} \int_0^{2\pi} dt \frac{\partial P}{\partial z} cos(kt). \tag{17}$$

These equations are the Fourier transform of the differential equations of motion, but for our steepest descent gradient method of solution it is essential to recognize that these equations determine also an extrema of the

action integral, Eq. 7, even when only a *finite* number of Fourier terms in the expansion the the orbital coordinates are taken into account. For convergent Fourier expansions, the number of such terms depends, of course, on the desired numerical accuracy for the solutions. Starting with the Fourier coefficients to some approximate form of the periodic orbit, and evaluating the partial derivatives of the action, Eqs. 12 -14, an improved orbit is then obtained by changing the value of each coefficient in proportion to the corresponding partial derivative of the action. For example, with some suitable initial values for the coefficient $a(k_o)$, $b(k_e)$ and $c(k_e)$, we obtain a new value $a'(k_o)$ by the transformation

$$a'(k_o) = a(k_o) + \frac{\delta s}{u(k_o)} \frac{\partial A}{\partial a(k_o)}, \tag{18}$$

with similar expressions for the other Fourier coefficients $b(k_e)$ and $c(k_e)$, where δs is a parameter. Then, to first order in the difference $\delta a(k_o) = a'(k_o) - a(k_o)$, the change δA in the action integral is given by

$$\delta A = \delta a(k_0) \frac{\partial A}{\partial a(k_o)} = \frac{\delta s}{u(k_o)} (\frac{\partial A}{\partial a(k_o)})^2. \tag{19}$$

The sign of the parameter δs must be chosen to be positive (negative) depending on whether the action is a maximum (minimum) with respect to the variation $\delta a(k_o)$. This procedure is then iterated until the partial derivatives of the action are reduced to any desired accuracy. Of course, the sign of δs is not known a-priori, but if the wrong value is chosen, one finds that the iteration diverges. Our method differs in an important way from the standard method of steepest descent by the introduction of the factor $1/u(k)$ in Eq. 18, which is important to obtain convergence with moderate values of the paramater δs (in the range 0.05 to 0.1). In this range most of our calculations have converged after a a few hundred interations to values for $\delta a = a'(k_o) - a(k_o)$ of order 10^{-10} to 10^{-13}, and similar for the other Fourier coefficients. However, near the limit $\Omega = 1$, which corresponds to the Lagrange circular orbit, we found that about 10^4 to 10^5 iterations were necessary to obtain convergence of the dominant Fourier coefficient $a(1)$ to only few decimal places. The reason for this very slow convergence turns out be that in the Lagrange limit, the transformation given by Eq. 18 has a marginal eigenvalue, which will be discussed in the next section. For a

frame rotating around the x axis of symmetry, we found that the various extrema of the action integral always occur at a *minimum* of this integral for variations with respect to the Fourier coefficients shown in Figs. 4-6, but for rotations around the y axis, the extrema with respect to the coefficients $c(1)$ and $c(3)$ occurred at a *maximum* of the action integral. For rotations around the y axis of symmetry of the figure eight (see Figs. 8 and 9), we found that for Ω somewhat greater than 0.8, the iterations of our Fourier gradient transformation diverged, suggesting the existence of a nearby singularity in the dependence of the corresponding family of solutions as a function of Ω.

II. Perturbation Solution Near the Lagrange Circular Orbit

To illustrate the application of our steepest descent Fourier gradient transformation, Eq.18, we calculate analytically the integrals in Eqs. 15-17 near the Lagrange solution for $\Omega = 1$. Setting $\epsilon = a(1)/r$, $b_2 = b(2)/r$, and $b_4 = b(4)/r$ where $r = 1/3^{1/6}$ is the length scale for $m = 1$, we evaluate these integrals by perturbation theory to first order in $\beta = 1 - \Omega$, and obtain the following transformations for the coefficients ϵ, b_2 and b_4:

$$\epsilon' = \frac{\epsilon}{b_2^3}(1 - \frac{9}{8}\epsilon^2 + \frac{3}{2}b_4), \tag{20}$$

$$b_2' = (4(1-\beta)b_2 + \frac{1}{b_2^2}(1 - \frac{3}{4}\epsilon^2))/(5 - 2\beta), \tag{21}$$

and

$$b_4' = (8(1-\beta)b_4 + \frac{1}{b_2^2}(\frac{3}{8}\epsilon^2 - b_4))/(17 - 2\beta). \tag{22}$$

The fixed points for these transformations are given by

$$\epsilon_f = \sqrt{\frac{19}{3}\beta}, \tag{23}$$

$$b_{2f} = 1 - \frac{9}{4}\beta, \tag{24}$$

and

$$b_{4f} = \frac{1}{4}\beta. \tag{25}$$

These fixed points correspond to the lowest order perturbation solution near the Lagrange circular orbit, previously obtained by C. Marchal [4], [5], except for the sign for b_{4f}, which is given incorrectly in these references.

It is illuminating to calculate the first order deviations $\delta\epsilon = \epsilon - \epsilon_f$, $\delta b_2 = b_2' - b_{2f}$ and $\delta b_4 = b_4' - b_{4f}$, which satisfy the simpler equations

$$\delta\epsilon' = \delta\epsilon(1 - 4\beta - 6\sqrt{3\beta/19}\delta\epsilon), \tag{26}$$

$$\delta b_2' = \frac{2}{5}(1 - \frac{42}{5}\beta)\delta b_2, \tag{27}$$

$$\delta b_4' = \frac{15}{34}(1 - \frac{274}{255}\beta)\delta b_4. \tag{28}$$

Evidently, in the Lagrange limit where β vanishes, iterations of δb_2 and δb_4 converge rapidly to the respective fixed points, while the transformation for ϵ, Eq. 26, has an eigenvalue which approaches unity, and therefore converges increasingly slowly as β decreases. This property explains the slow convergence which we found for iterations of the exact transformations near the Lagrange limit. For example, if one wishes to determine the fixed point to an accuracy $\delta = 10^{-m}$, then the number of iterations required for this map is $n \approx 2.3 * m/4\beta$. For example, to obtain ϵ_f for $\beta = .0001$ to an accuracy $\delta = 10^{-4}$, which gives $\epsilon_f = .025166$, one needs approximately $n = 23,000$ iterations of these linearized equations.

III. Numerical results

In this section we present our numerical results in graphical form for finite-angular momentum figure eight shaped orbits in a rotating frame with angular frequency Ω. These orbits are obtained by the steepest descent gradient Fourier method described in section I. For rotations along the horizontal symmetry axis (x-axis) of the planar figure eight orbit, the values of Ω are in the range 0 to 1. As an illustration of the characteristic shape of such orbits in the rotating frame, we show in Fig.1 a three dimensional finite angular momentum periodic orbit for three equal masses in a frame rotating with frequency $\Omega = 0.5$. The shape of this orbit corresponds to a three dimensional figure eight which is bend symmetrically downward at a self-crossing point of the orbit that lies on the z axis at $x = y = 0$, as can be seen from Eqs.1-3. The position of each of the three masses is shown at five equal intervals

during a third of the period $\tau = 2\pi$, in corresponding segments of the orbit indicated by blue, red and green colors. The segments of the orbit below the $x - y$ plane are indicated by dashed lines. For positive values of x this orbit is transversed clockwise as viewed on a projection on the $x - y$ plane, while for negative values of x it is transversed counterclockwise, where the entire frame is rotating counterclockwise around the x-axis with respect an inertial frame.

We have obtained similar orbits for an odd number of equal masses $n \geq 3$. A typical case for a finite angular momentum orbit with 21 masses is shown in red in Fig. 2, while the associated planar figure eight orbit for $\Omega = 0$ is shown in blue, and the Lagrange circular orbit for $\Omega = 1.0$ is shown in green. In Fig. 3 we show the projection on the $x-y$ plane of six of these orbits, with $n = 3$ and $\Omega = 0, 0.2, 0.4, 0.6, 0.8$ and 1.0, corresponding to similar figures in [6]. In Figs. 4-6, we plot the first few Fourier coefficients of the expansion of the coordinates for the finite angular momentum figure eight solution, Eqs. 1-4, as a function of the angular frequency Ω, which give numerical evidence that these coefficients are continuous functions of Ω between $\Omega = 0$, for the coefficients for the planar figure eight orbit, and $\Omega = 1$, for the coefficient of the classical Lagrange orbit. We show with dashed lines Marchal's perturbation approximation for these coefficients [4],[5] near the Lagrange limit $\Omega = 1$, evaluated to second order in powers of the square root of $\beta = 1 - \Omega$, and also our corresponding expansion to second order in powers of Ω near $\Omega = 0$ for the bifurcation near the planar figure eight orbit [3]. In Fig. 7 we show graphically a numerical difference approximation, $\Delta(coefficient)/\Delta\Omega$, to the derivative of the first three Fourier coefficients with respect to Ω, where $\Delta\Omega = .005$. This figure gives further numerical evidence for the continuity of these coefficients as a function of ω (if discontinuities or jumps were present, these would be magnified in this calculation).

We have previously evaluated also some orbits for finite angular momentum of the figure eight orbit rotating about its other two symmetry axes [3], and recently existence proofs and further numerical results [6] have extended this work. In Fig. 8 we show an orbit for rotation about the y axis with $\Omega = 0.5$. In this case the orbit does not cross at $x = y = 0$; instead the two values of z are equal but opposite in sign as can be readily seen from Eqs. 1,2 and 4. In Fig. 9 we show the projection of these orbits on the $x - y$ plane for $\Omega = 0., 0.2, 0.4, 0.6$ and 0.8, corresponding to similar results in [6]. This result indicates that in this case the projected crossing angle at $x = y$

is a constant. But for values of Ω greater than about 0.8 we found that our iteration procedure ceases to converge, suggesting that there is a singularity in the dependence of these coefficient on Ω. Finally, we give in Fig.9 an illustration of the shape of the orbit when the axis of rotation is normal to the plane of the figure eight orbit, similar to one shown in [3]. In this case the finite angular momentum orbit remains planar but the symmetry about the y axis is broken.

We remark that our steepest descent gradient method also converges when the axis of the rotating frame is not taken along any of the symmetry axes of the planar figure eight orbit, but this procedure does not generate new solutions. In this case one has to take into account additional terms in the Fourier expansion of the coefficients of the orbit, and the previous separation into even and odd integers in the sums, Eqs. 1-4 is no longer valid. We find that for not too small values of Ω, the iterations converge to a solution which correspond to a member of the family associated with rotations along the horizontal symmetry axis of the figure eight orbit, which is now located along the chosen rotation axis. But as Ω approaches 0 the convergence of the iterations becomes extraordinarily slow; e.g. for $\Omega = .01$ one requires about 10^6 iterations to achieve convergence.

IV Nonlinear Stability

In this section we present numerical results for the stability of the three families of periodic figure eight orbits with finite angular momentum along the three symmetry axis of the eight. We also give some examples of stable orbits located in the vicinity of these orbits near the critical point where the periodic orbits of a family become unstable. To determine the stability of a periodic orbit we calculate it numerically with the fourth order Runge-Kutta algorithm, taking as initial coordinates and momenta values very close to those obtained from our Fourier gradient method (see section I). We then follow this orbit for up to approximately 10^3 periods monitoring the constancy of the total energy and the total angular moment to an accuracy 10^{-5}. For the family of orbits rotating around the horizontal axis of symmetry of the eight, a linear stability analysis in reference [6], reported that these orbits are linearly unstable for all finite angular frequencies $\Omega > 0$. We find, however, that for Ω approximately less than 0.1 the orbits bifurcate into *stable* albeit quite complex quasi-periodic orbits. An example for such a

stable nearby orbit for $\Omega = .05$ is shown in Fig. 11, which is plotted for 40 periods. Each of the the three equal masses moves on separate but nearby orbits indicated by the colors blue, red and green. As the number of periods increases, further wings appear and the orbit starts to fill a spherical volume with the radius of half the horizontal axis of the figure eight orbit. Evidently, in this case the linear stability analysis given in reference [6] is inadequate to determine the domain for the existence of stable orbits in the vicinity of this family. But for the family of periodic figure eight orbit rotating around the y and the z axis, our numerical stability results are in accordance with the the linear analysis [6]. As an example, in Fig. 12 we show a quasi-periodic period orbit for $\Omega_y = .09$ for 166 periods. We have checked for 333 periods that for $\Omega_y = .0920$ such an orbit remain stable, while for larger values of Ω_y it becomes unstable. Likewise, for rotations around the z axis of symmetry of the eight we found nearby quasi-periodic orbits for $\Omega_z < .585$ which we verified to remain stable for 333 periods. For $\Omega_y = .55$ an example is shown in Fig. 12 for 20 periods. These orbits correspond to a slow precesion with small deformations of the stable orbit shown in Fig. 10.

Acknowledgements

I would like to thank C. Marchal for his comments.

References

[1] Moore C.: 1993, 'Braids in classical gravity', *Physical Review Letters* **70**,3675-3679.

[2] Chenciner A. and Montgomery R.: 2000, 'A remarkable periodic solution of the three body problem in the case of equal masses' *Annals of Mathematics***152**: 881-901.

[3] Nauenberg M.:2001, 'Periodic orbits for three particles with finite angular momentum' *Physics Letters* **292** 93-99.

[4] Marchal C.:1990, '*The three body problem* Elsevier Science Publishers B.V. pp 251-257

[5] Marchal C.:2001, 'The family P_{12} of the three body problem-The simplest family of periodic orbis, with twelve symmetries per period', *Celestial Mechanics and Dynamical Astronomy* **78**, 279-298.

[6] Chenciner A., Fejoz J. and Montgomery R.:2004 'Rotating eights I: the three Γ_i families (unpublished)

[7] Chenciner A., Gerver J., Montgomery R. and Simo C.: "Simple Choreographic Motions of N bodies: A preliminary study' (unpublished)

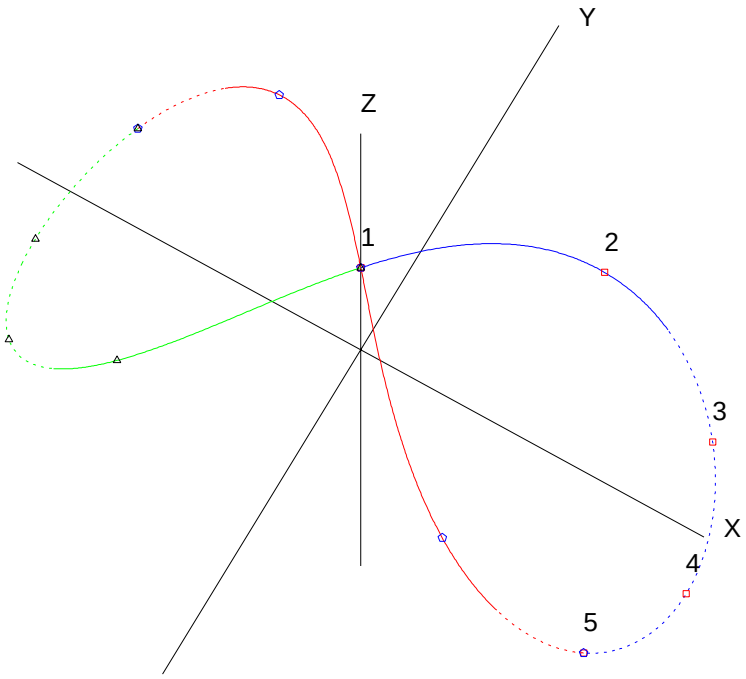

Figure 1: Finite angular momentum figure eight orbit, which is periodic in a frame rotating around the $x - axis$ with frequency $\Omega = 0.5$. The position of the three masses are indicated by squares at 4 equal time intervals during 1/3 of a period.

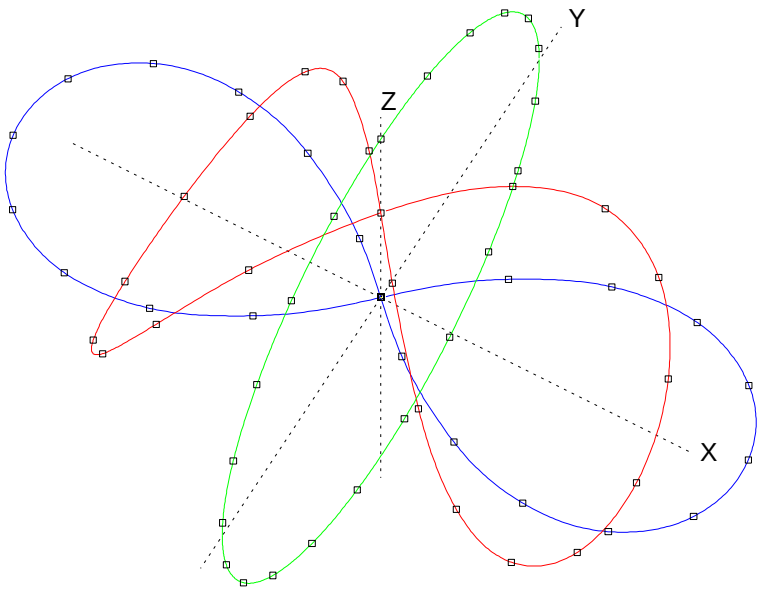

Figure 2: Periodic orbits with 21 particles of equal mass shown at equal time intervals indicated by squares. The blue curve is the planar figure eight orbit in the $x-y$ plane, the green curve is the circular Lagrange orbit in the $y-z$ plane , and the red orbit is a member of a family of finite angular momentum figure eight orbits which is periodic in a frame rotating with frequency $\Omega = 0.5$ around the x-axis.

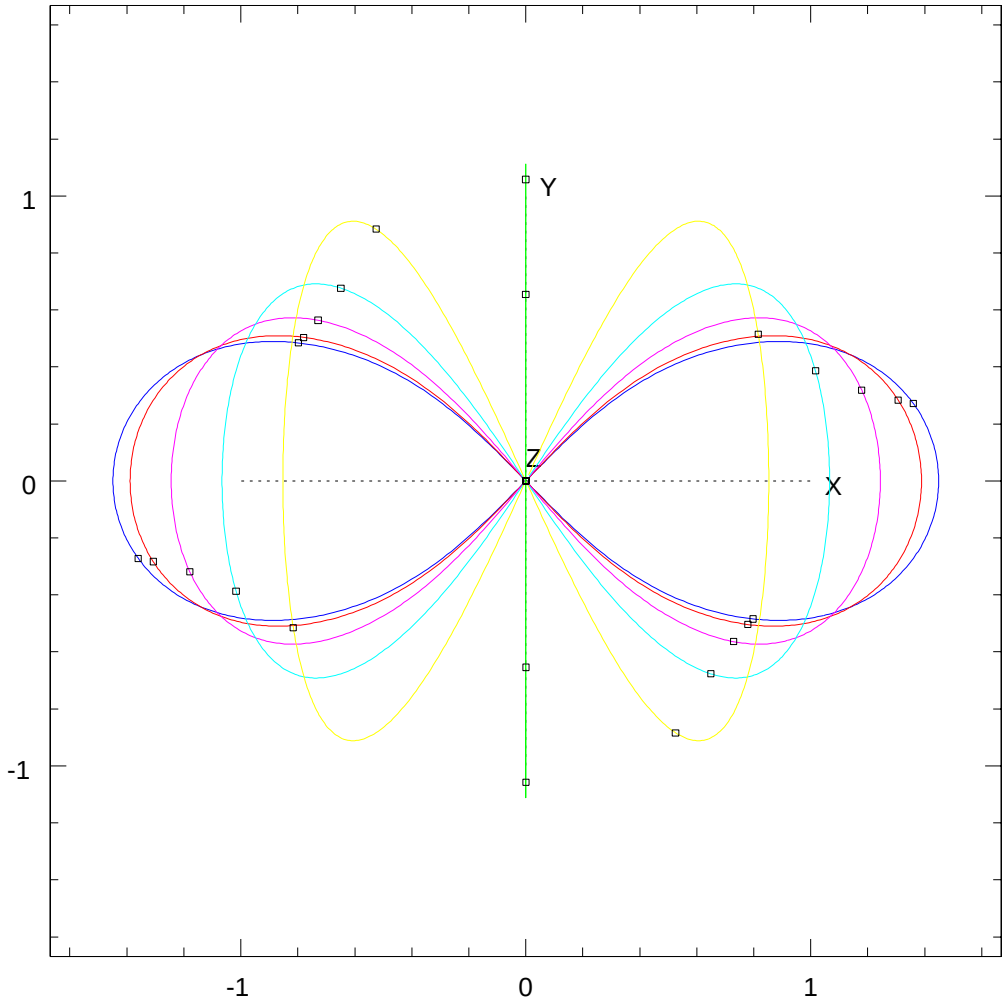

Figure 3: Projection on the $x-y$ plane of finite angular momentum figure eight orbits for three equal masses rotating shown in a frame around the x-axis of symmetry for $\Omega = 0, 0.2, 0.4, 0.6, 0.8$ and 1.0 (from blue to green).

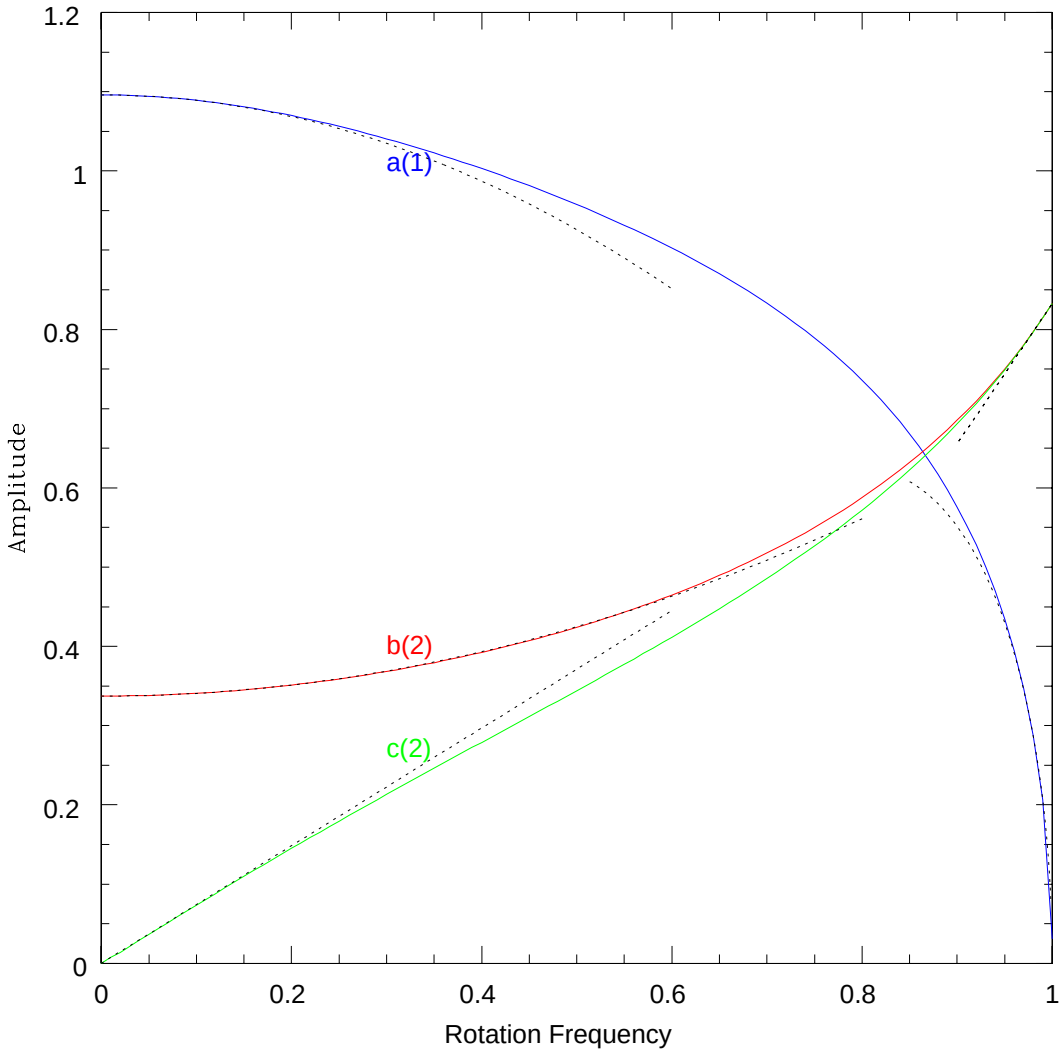

Figure 4: First three Fourier coefficients for the finite angular momentum figure eight solutions as functions of the rotation frequency Ω. The dashed curves are perturbation solutions.

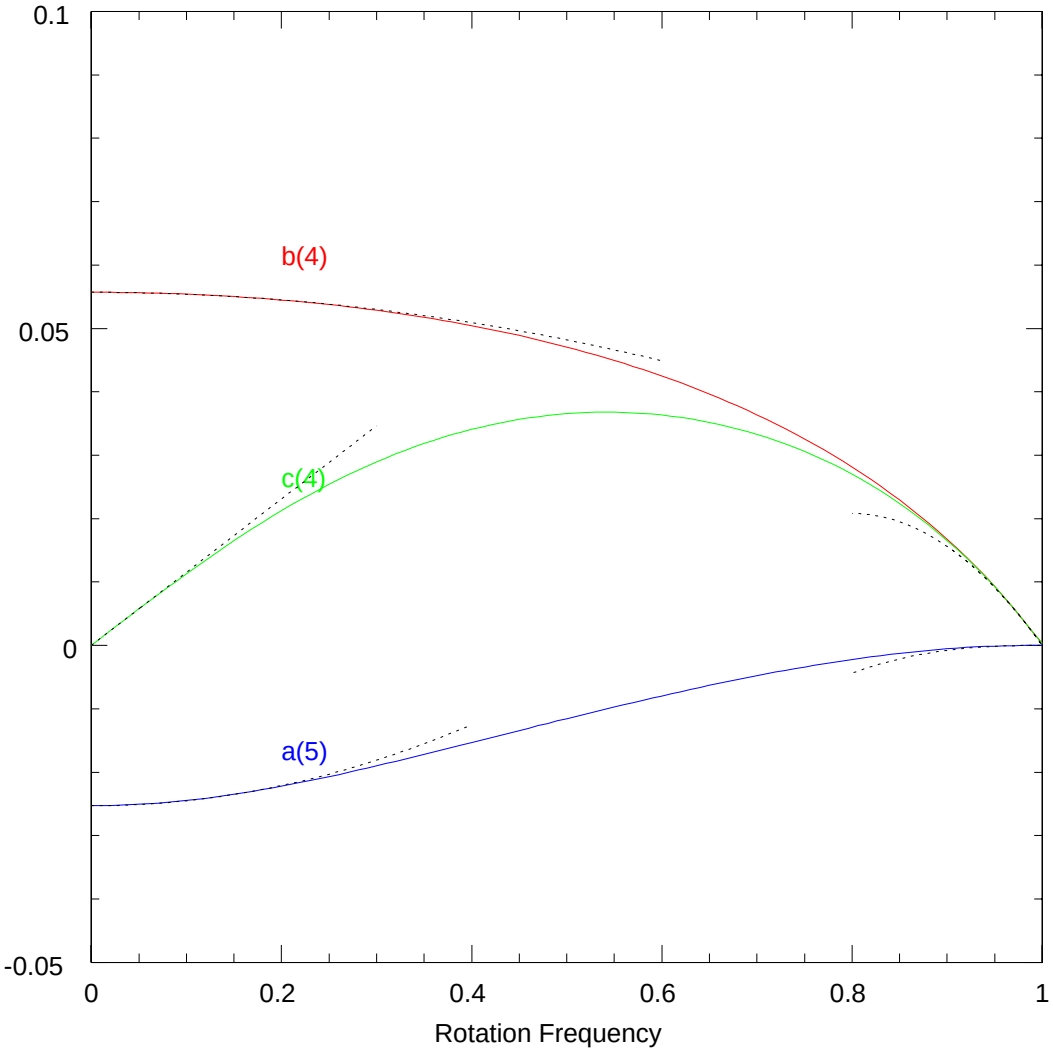

Figure 5: Fourier series coefficients for the finite angular momentum figure eight solutions as functions of the rotation frequency Ω. The dashed curves are perturbation solutions (see text)

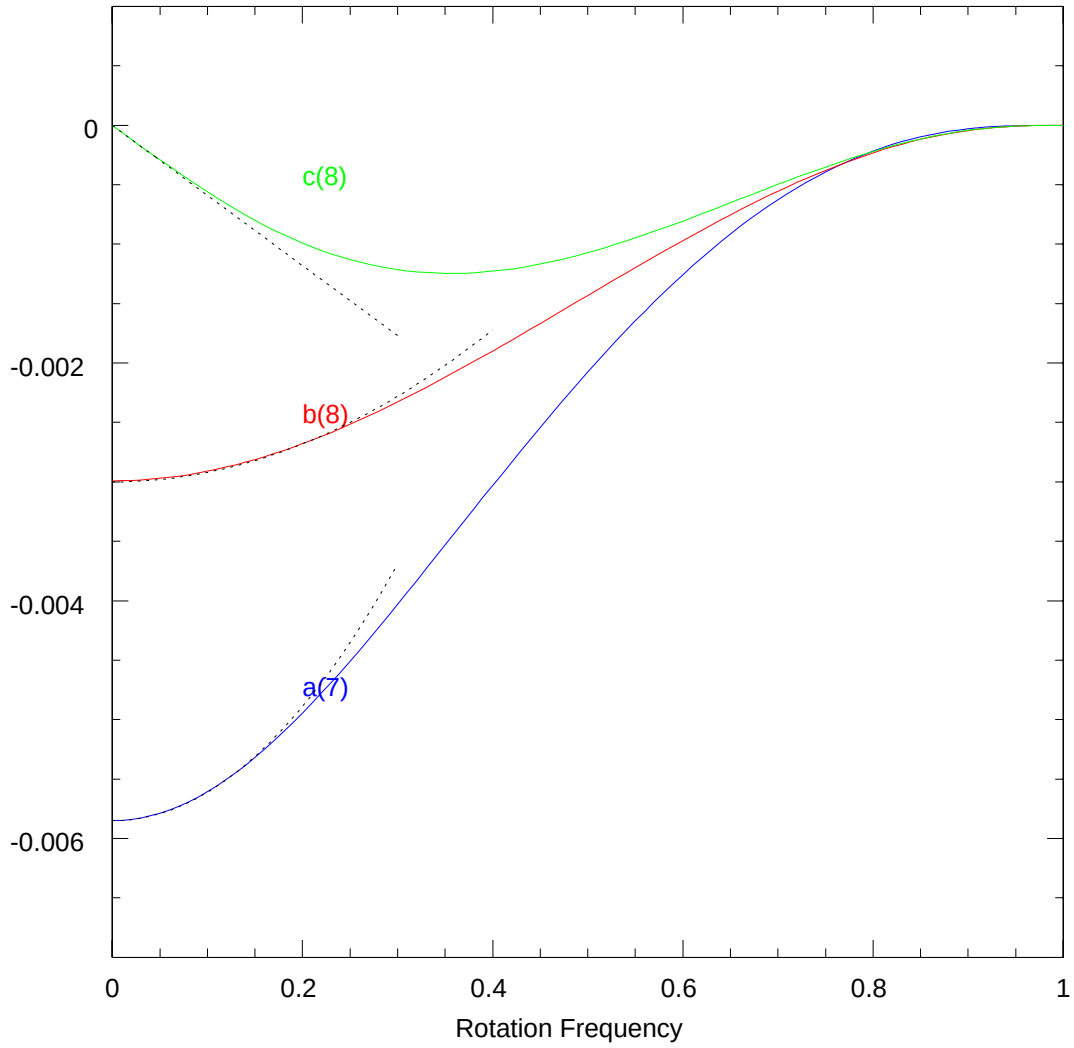

Figure 6: Fourier series coefficients for the finite angular momentum figure eight solutions as functions of the rotation frequency Ω. The dashed curves are perturbation solutions.

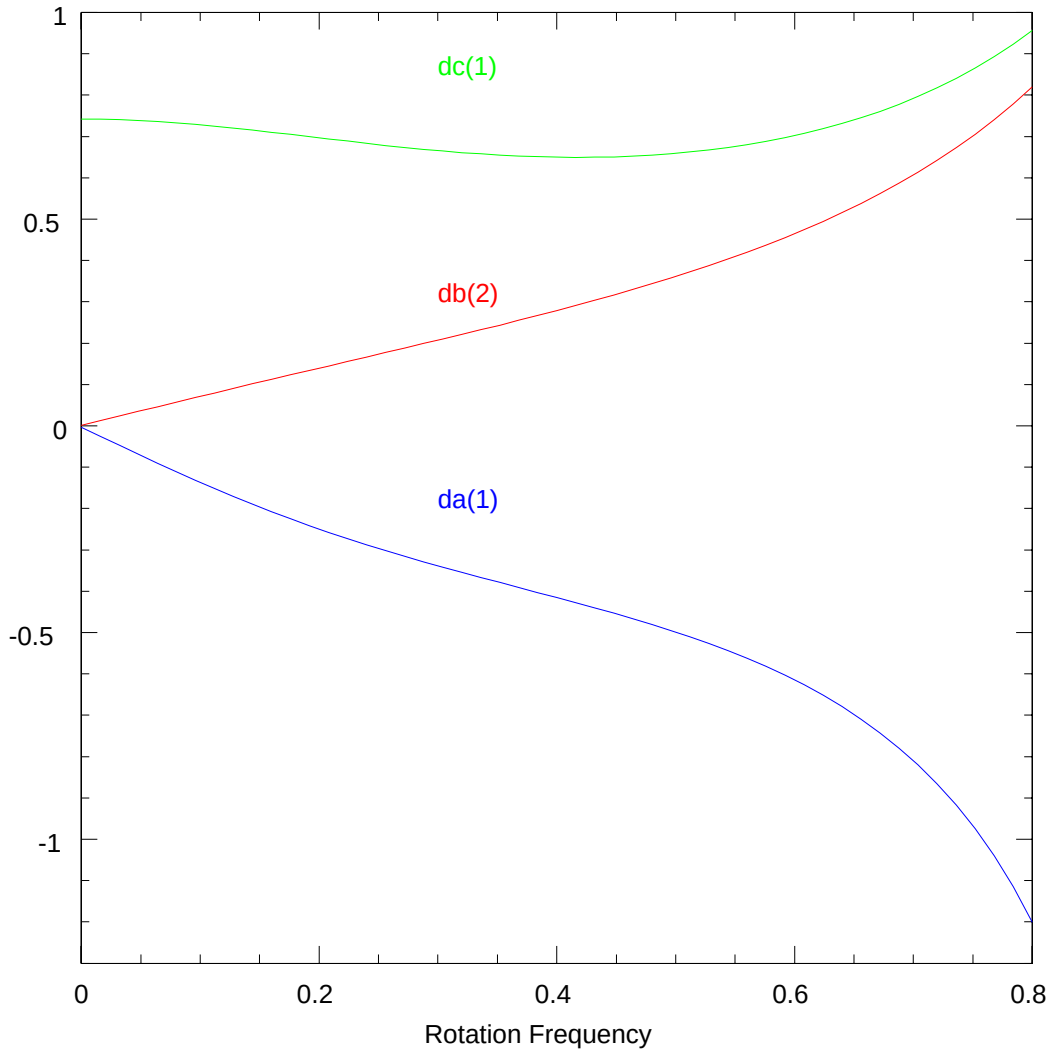

Figure 7: Numerical derivative with respect to the rotation frequency Ω of the first three Fourier coefficients for the finite angular momentum figure eight solutions as functions of the rotation frequency Ω.

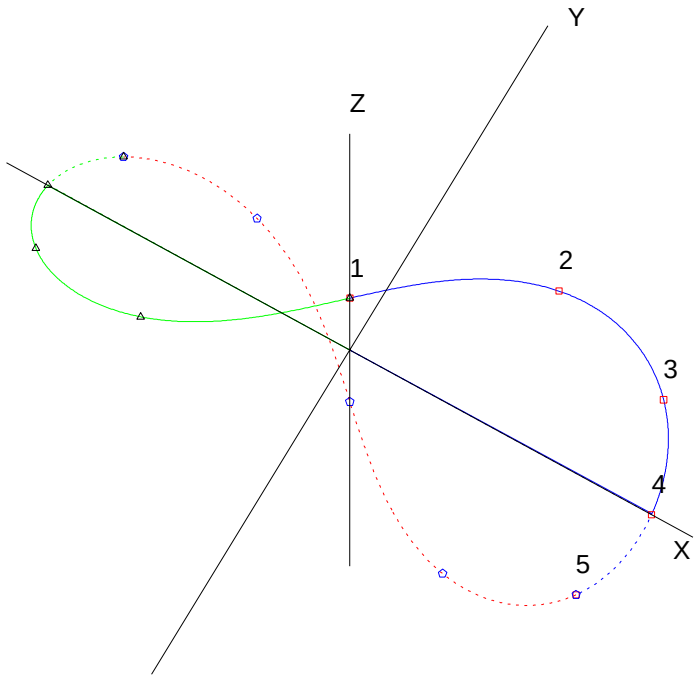

Figure 8: Finite angular momentum figure eight orbit rotating around the y axis of symmetry for $\Omega = 0.5$. The position of the three masses are indicated by squares at 4 equal time intervals during 1/3 of a period.

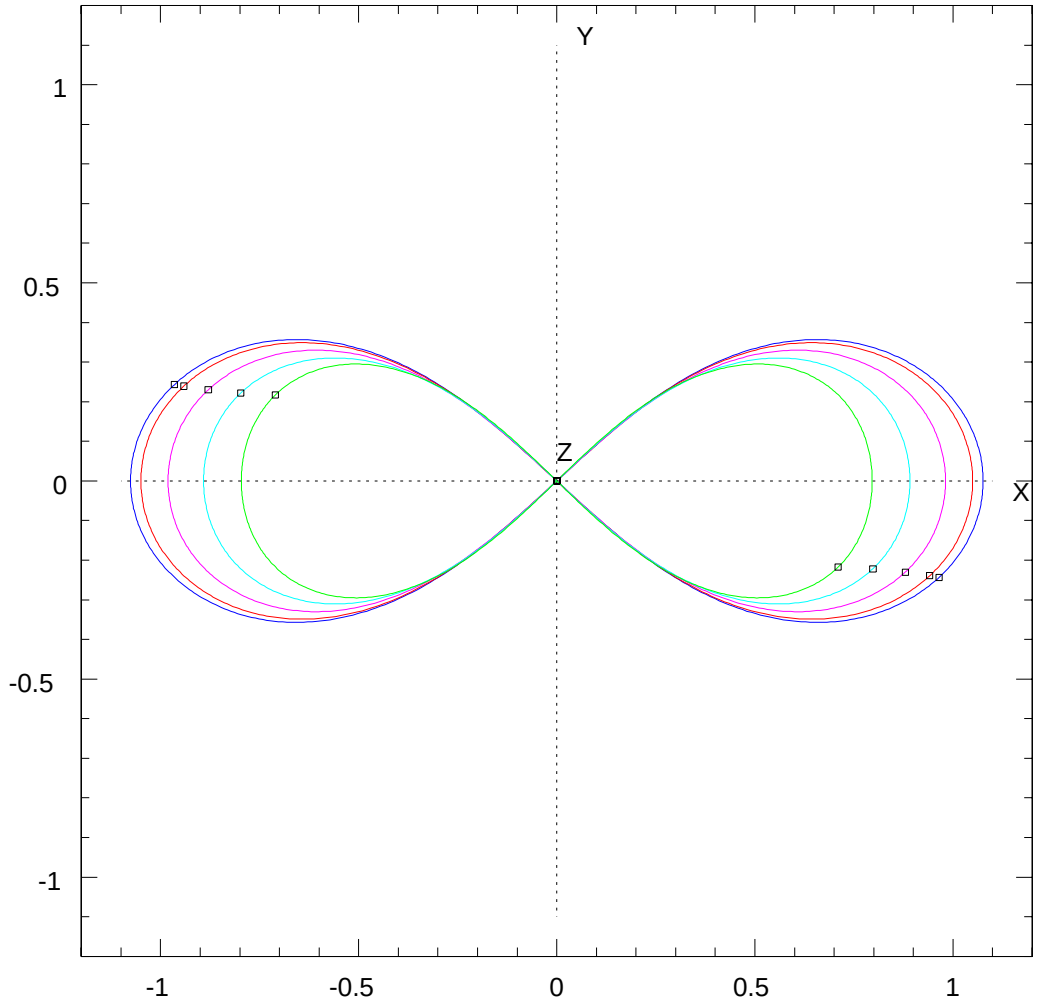

Figure 9: Projection on the $x - y$ plane of finite angular momentum figure eight solutions shown in a frame rotating around the y axis for $\Omega = 0, 0.2, 0.4, 0.6$, and 0.8 (from blue to green).

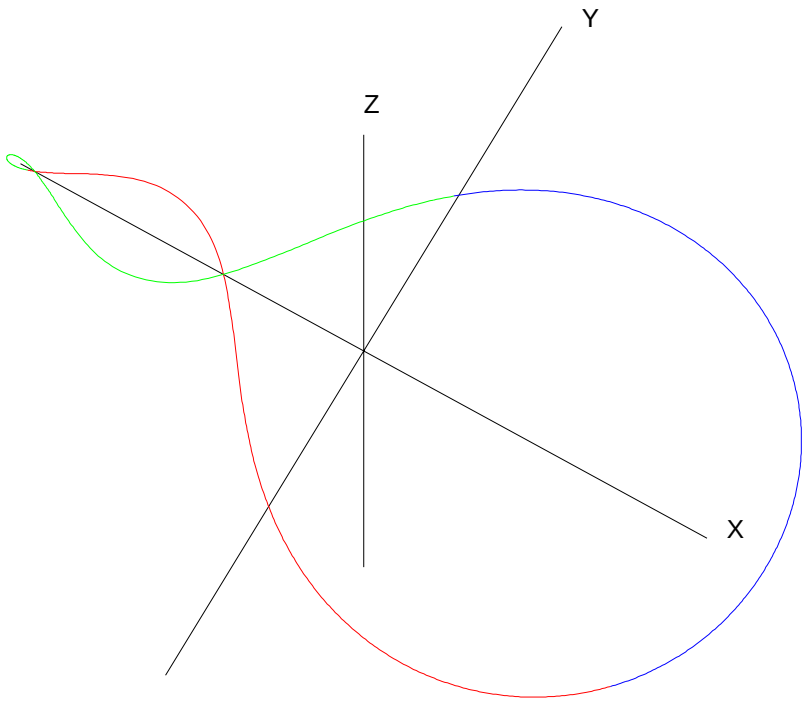

Figure 10: Figure eight orbit rotating around the z axis with $\Omega = .5$. The blue,red and green segments are the trajectories for three equal masses during one third of a period.

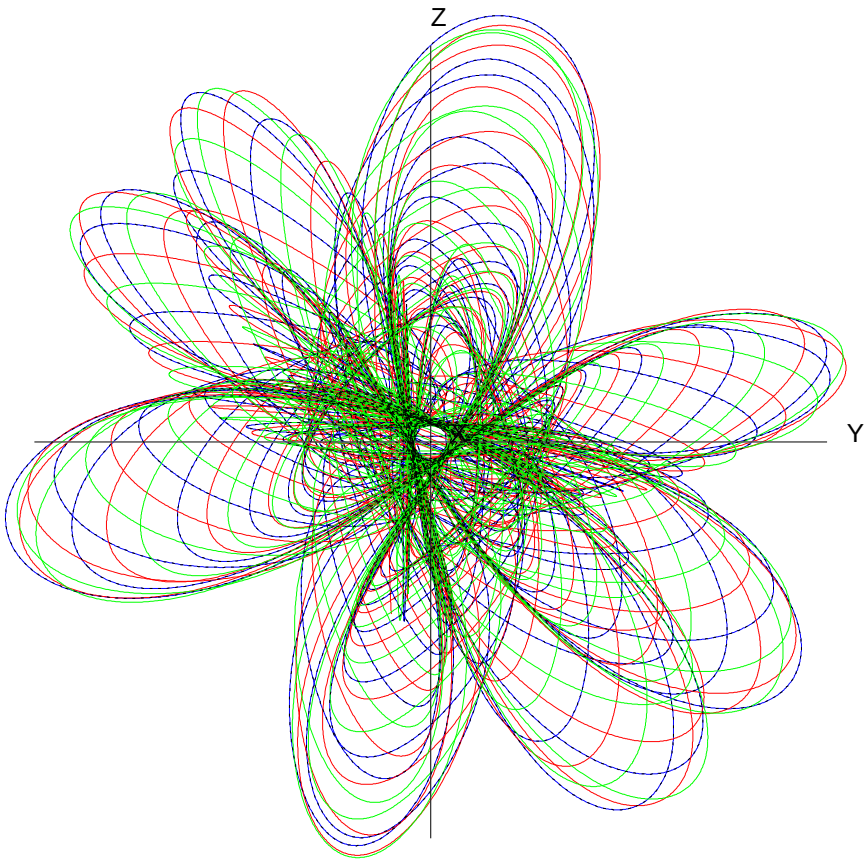

Figure 11: Stable figure eight orbit in a rotating frame around the x axis with $\Omega = .05$. The blue,red and green orbits are the separate trajectories for three equal masses. during 40 orbits

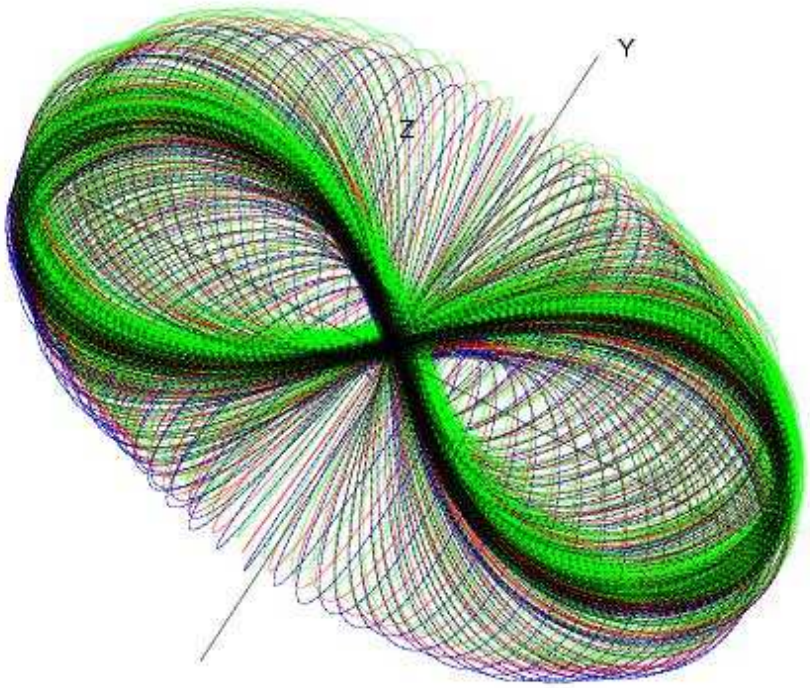

Figure 12: Stable figure eight orbit in a rotating frame around the y axis with $\Omega = .05$. The blue,red and green orbits are the separate trajectories for three equal masses during 166 orbits

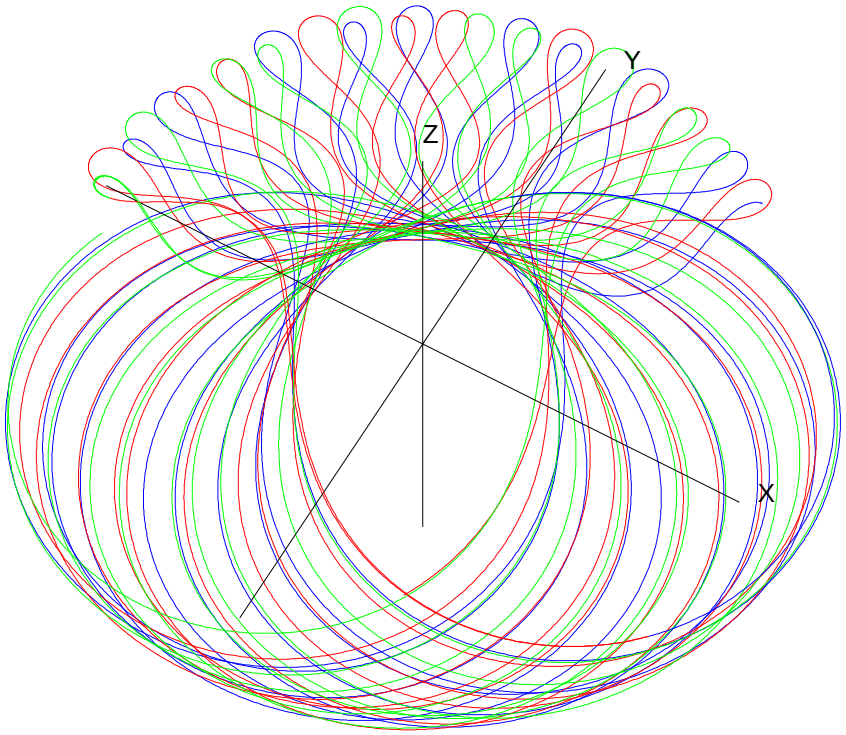

Figure 13: Stable figure eight orbit in a rotating frame around the z axis with $\Omega = .55$. The blue,red and green orbits are the separate trajectories for three equal masses.